Chaos in low-dimensional Lotka–Volterra models of competition

J A Vano, J C Wildenberg, M B Anderson, J K Noel and J C Sprott

Department of Physics, University of Wisconsin–Madison, Madison, Wisconsin 53706, USA

Abstract
The occurrence of chaos in basic Lotka–Volterra models of four competing species is studied. A brute-force numerical search conditioned on the largest Lyapunov exponent (LE) indicates that chaos occurs in a narrow region of parameter space but is robust to perturbations. The dynamics of the attractor for a maximally chaotic case are studied using symbolic dynamics, and the question of self-organized critical behaviour (scale-invariance) of the solution is considered.

1. Introduction

Originally derived by Volterra in 1926 to describe the interaction between a predator species and a prey species [1] and independently by Lotka to describe a chemical reaction [2], the general Lotka–Volterra model is the starting point for a wide variety of models in ecology, biology, economics, chemistry, physics, etc [3]. The natural processes to which the models are typically applied usually exhibit aperiodic fluctuations. On the other hand, the models, although widely studied, usually have static or periodic solutions. In those few instances where chaos is observed in the models, it has not been extensively explored. We consider here the simplest form of such a system in which N species (or agents in a financial model) with population x_i for $i = 1$ to N compete for a finite set of resources according to

$$\frac{\mathrm{d}x_i}{\mathrm{d}t} = r_i x_i \left(1 - \sum_{j=1}^{N} a_{ij} x_j\right). \tag{1}$$

Here the r_i represents the growth rate of species i and a_{ij} represents the extent to which species j competes for resources used by species i. Equation (1) can also be viewed as the first approximation in a Taylor-series expansion for a wide class of models [4], and so it is rather more general than it might at first appear.

Imposing the additional conditions

$$r_i > 0, \tag{2a}$$

$$a_{ij} \geqslant 0 \tag{2b}$$

leads to models for competitive species in which each species or agent competes for a finite set of resources. These conditions also ensure that all solutions with non-negative initial conditions have the highly desirable feature that they remain bounded and asymptotically approach the region $0 \leqslant x_i \leqslant 1$.

In 1976 Smale [5] demonstrated that, under conditions (2a) and (2b), any asymptotic dynamic behaviour is possible for populations of five or more species, i.e. $N \geqslant 5$. In contrast, Hirsch [6–11] has demonstrated that considerable structure remains in the solutions. In particular, there exists a closed invariant set C which is homeomorphic to the $(N-1)$-dimensional simplex $\Delta_{N-1} = \{x_i : x_i \geqslant 0, \sum x_i = 1\}$ which is a global attractor for every point (excluding the origin) in the domain $D = \{x_i : x_i \geqslant 0\}$. The set C is known as the carrying simplex since it 'carries' all of the asymptotic dynamics of equation (1), and its existence significantly reduces the possible asymptotic dynamics. For example, for three or fewer species, i.e. $N \leqslant 3$, no chaotic solutions are possible, and hence models with four species, i.e. $N = 4$, are the simplest examples where chaotic behaviour is possible.

In this paper, we explore the occurrence of chaotic solutions for a four-species competitive Lotka–Volterra model. To begin, without loss of generality, we can reduce the 20-dimensional parameter space of r_i and a_{ij} as follows. By measuring the population of each species in units of its carrying capacity (as measured in the absence of the other species), the self-interactions terms a_{ii} can be set to 1. By measuring time in units of the inverse growth rate of species 1, the growth rate r_1 of species 1 can be set to 1. In the remaining 15-dimensional parameter space we employ a brute-force numerical search to seek out parameter values that exhibit chaotic solutions. While such solutions appear to be relatively rare in this vast parameter space, values such as

$$r_i = \begin{bmatrix} 1 \\ 0.72 \\ 1.53 \\ 1.27 \end{bmatrix}, \qquad a_{ij} = \begin{bmatrix} 1 & 1.09 & 1.52 & 0 \\ 0 & 1 & 0.44 & 1.36 \\ 2.33 & 0 & 1 & 0.47 \\ 1.21 & 0.51 & 0.35 & 1 \end{bmatrix} \tag{3}$$

can be found that produce chaotic solutions and appear to be robust to small perturbations of the parameters.

The case above represents an attempt to maximize the largest LE relative to the geometric mean of the growth rates $(r_1 r_2 r_r r_4)^{1/4}$, subject to the constraint that none of the variables x_i falls below 0.001, which in a real ecology mitigates against a species becoming extinct. In addition, three of the matrix elements whose values were small were fixed at zero. The corresponding largest LE is $\lambda_1 \approx 0.0203$, and the sum of all the exponents is $\sum \lambda_i \approx -1.2834$, implying a predictability horizon on the order of 50 growth times of a typical species and strong dissipation.

It is interesting to note that the chaotic solutions found in such brute-force searches all appear to exploit the same mechanism used by Arneodo *et al* to construct chaotic three-dimensional predator–prey Lotka–Volterra systems [12] and four-dimensional competitive Lotka–Volterra systems [13]. However, since our search was not constrained to cases with all r_i equal, we are able to exhibit chaotic solutions in settings in which each of the four species has its own distinct growth rate. Thus we believe that the system studied here is the simplest example of chaos in a realistic competitive Lotka–Volterra model and that it is near maximally chaotic for such a system with only four species.

2. Summary of lower-dimensional dynamics

One interesting feature of the Lotka–Volterra system in equation (1) is that if the population of any species vanishes, i.e. if $x_i = 0$, then that species will remain extinct and the remaining species will follow a lower-dimensional Lotka–Volterra system, i.e. equation (1) with a smaller N. Thus the boundary of the set of N coexisting species is made up of sets of $N - 1$ coexisting species, which is again made up of sets of $N - 2$ coexisting species, and so on. As such, it is useful to review what is known about the Lotka–Volterra systems in equation (1) with a small number of species.

For the single-species case, i.e. $N = 1$, equation (1) reduces to the Verhulst equation [14]

$$\frac{\mathrm{d}x}{\mathrm{d}t} = x(1 - x)$$

and solutions for all initial conditions $x(0) > 0$ are asymptotic, as $t \to \infty$, to the stable equilibrium at $x = 1$.

In the two-species case, i.e. $N = 2$, there is a coexisting equilibrium at the fixed point

$$x_1 = (1 - a_{12})/(1 - a_{12}a_{21}),$$

$$x_2 = (1 - a_{21})/(1 - a_{12}a_{21}).$$

If both a_{12} and a_{21} are less than 1, this fixed point is stable, and all initial conditions asymptotically approach not only the closed, invariant, attracting, one-dimensional carrying simplex but also the fixed point. If either a_{12} or a_{21} is greater than 1, this fixed point is a saddle point, and all non-negative initial conditions (other than the fixed points) asymptotically approach the closed, invariant, attracting, one-dimensional carrying simplex (which is the unstable manifold of the coexisting fixed point) and flow, by the principle of competitive exclusion [15], towards the boundary with one species approaching extinction.

For three species, if condition (2b) is relaxed, chaotic solutions of equation (1) are possible for appropriate choices of a_{ij} [12]. However, under the competition hypothesis (2b) the presence of the closed, invariant, attracting, two-dimensional carrying simplex implies, by the Poincare–Bendixson theorem [16], that the only asymptotic dynamics are fixed points, periodic orbits [17–19] or limit cycles [20] consisting of boundary fixed points connected by heteroclinic orbits (e.g. with $r_1 = r_2 = r_3 = 1$, $a_{12} = a_{23} = a_{31} = \alpha$, $a_{13} = a_{21} = a_{32} = \beta$ and $\alpha + \beta = 2$).

In the case of four species, Arneodo *et al* [13] have demonstrated how one might construct a chaotic solution with parameters satisfying conditions (2a) and (2b) by using the transformation described by Coste *et al* [21], to embed a chaotic three-dimensional Lotka–Volterra system [12] (which does not satisfy conditions (2a) and (2b)) into a four-dimensional Lotka–Volterra system. In choosing the embedding they can ensure conditions (2a) and (2b). While this construction does produce an example of a four-species system with chaotic orbits, it does not address questions such as the prevalence of these chaotic ecologies or even their existence for unequal species growth rates, and it does not produce a maximally chaotic solution, all of which are addressed here.

3. Preliminary analysis

3.1. Equilibria and eigenvalues

For the remainder of the paper we consider the four-species case described in equation (3). There are $2^N = 16$ equilibrium points corresponding to taking either $x_i = 0$ or $(1 - \sum a_{ij}x_j) =$

0 for $i = 1, \ldots, N$. The former represents an equilibrium where species i is extinct while the latter represents one in which species i coexists with the other species.

The origin $x_1 = x_2 = x_3 = x_4 = 0$ is a repelling equilibrium with Jacobian matrix $\frac{\mathrm{d}\dot{x}_i}{\mathrm{d}x_j} = r_i$ for $i = j$ and $\frac{\mathrm{d}\dot{x}_i}{\mathrm{d}x_j} = 0$ for $i \neq j$. In contrast, let $\bar{x}$ denote the equilibrium point at which all species coexist with

$$\bar{x} \approx \begin{bmatrix} 0.3013 \\ 0.4586 \\ 0.1307 \\ 0.3557 \end{bmatrix}. \tag{4}$$

This fixed point is an index-2 spiral saddle whose Jacobian matrix

$$\frac{\mathrm{d}\dot{x}_i}{\mathrm{d}x_j} = -a_{ij} r_i x_i$$

has eigenvalues $0.0414 \pm 0.1903i$, -0.3342 and -1.0319.

We label the remaining 14 equilibrium points with the letter Q, using subscripts to denote which species are present (e.g. the equilibrium point at the origin is denoted simply by Q and the one at $\bar{x}$ is Q_{1234}). These equilibria can be classified as follows.

1. For the four equilibrium points that have only one species alive (Q_1, Q_2, Q_3 and Q_4) the population of the single alive species is at its carrying capacity, i.e. $x_i = 1$. These four equilibria are all saddle points.
2. Of the six equilibrium points with exactly two species alive, three (Q_{12}, Q_{14} and Q_{24}) have one of their x_i values negative and hence cannot be reached by a trajectory that starts with all x_i positive (i.e. they lie outside of D), while the remaining three (Q_{13}, Q_{23} and Q_{34}) lie on the boundary of D.
3. Of the four equilibrium points with exactly three species alive, only one (Q_{124}) does not have negative x_i values. It is an index-1 spiral saddle.

With the exception of the origin, the eight boundary equilibrium points (Q_1, Q_2, Q_3, Q_4, Q_{13}, Q_{23}, Q_{34} and Q_{124}), along with the coexisting fixed point $\bar{x}$, all lie in the carrying simplex which is homeomorphic to a tetrahedron as in figure 1. Furthermore, the four faces of the tetrahedron correspond to the two-dimensional carrying simplexes that arise in the three-dimensional Lotka–Volterra equations when $x_1 = 0$, $x_2 = 0$, $x_3 = 0$ or $x_4 = 0$, respectively. Figure 2 illustrates the dynamics that take place on these two-dimensional carrying simplexes. Note that the observed dynamics within the three-dimensional carrying simplex is very reminiscent of the chaotic three-dimensional Lotka–Volterra system constructed by Arneodo *et al* [12].

3.2. Chaotic attractor

Figure 3 shows that the attractor projected onto $x_1 x_2 x_3$ space is nearly two-dimensional with a folded-band structure reminiscent of the Rössler attractor [23], and figure 4 shows a representative portion of the time series of the four variables.

The LEs [24, 25] for this orbit are 0.0203, 0, -0.2748 and -1.0289, which implies a Kaplan–Yorke dimension [26] of $D_{KY} = 2.074$. The correlation dimension of Grassberger and Procaccia [27] was estimated using the extrapolation method of Sprott and Rowlands [28] with the result $D_2 = 2.066 \pm 0.086$, in good agreement with the Kaplan–Yorke dimension.

For the parameters in equation (3), the only attractor for initial conditions $x_i(0) > 0$ is the one in figure 3, and thus its basin of attraction is the entire domain of strictly positive
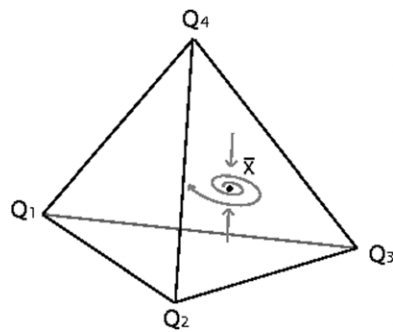
Figure 1. Carrying simplex for equation (1) with parameters in equation (3).
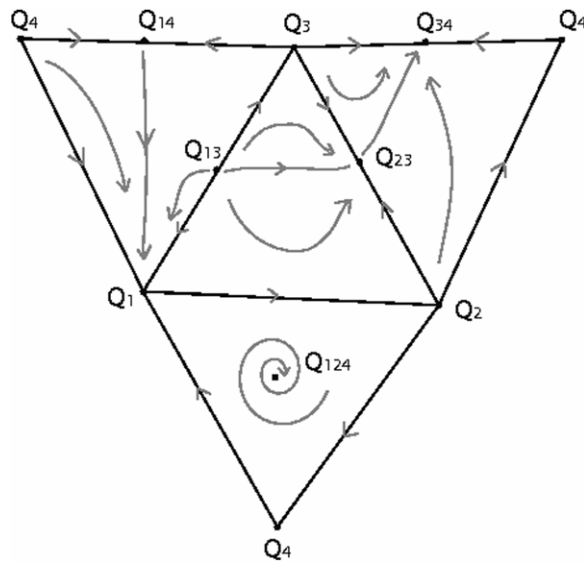

Figure 2. The dynamics on the boundary of the carrying simplex in figure 1. The tetrahedron has been unfolded and laid flat for better viewing.

populations (i.e. $x_i > 0$ for all i). However, some initial conditions cause x_3 to become very small for a long time before approaching the chaotic attractor, which in a real ecology would likely result in the permanent extinction of that species (and the suppression of chaos). Once on the attractor, the value of x_3 (the variable with the smallest minimum) never falls below 0.0019.

3.3. Homoclinic orbit

The stable and unstable manifolds originating from the coexisting equilibrium point $\bar{x}$ appear to intersect tangentially, resulting in a homoclinic connection which is shown in figure 5 projected onto the $x_1 x_2$ plane. Given the non-generic nature of a tangential intersection, it is difficult to verify these numerics, but the figure clearly suggests that there is at least one initial condition on the unstable manifold of the equilibrium that returns along the stable manifold to within the resolution of the plot. There is no reason to expect the equilibrium point to lie on the attractor,
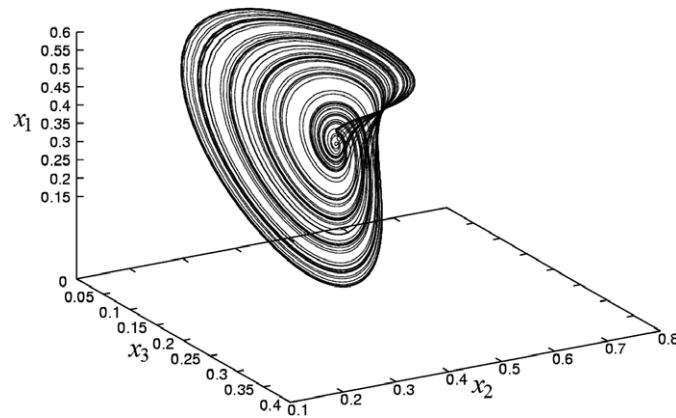
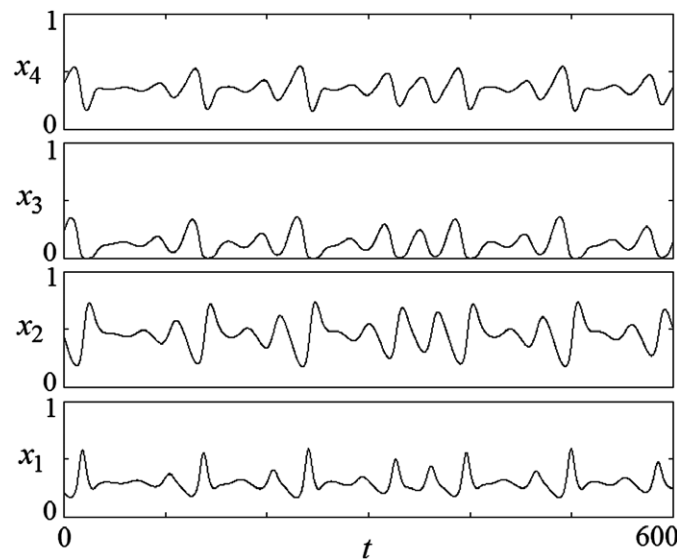**Figure 3.** Attractor projected onto $x_1 x_2 x_3$ space.

Figure 4. Time series for each species (vertical scale is 0 to 1).

but the trajectory on the attractor comes very close (a Euclidean distance of $<1 \times 10^{-4}$) to the equilibrium point, and hence the homoclinic connection also lies approximately on the attractor. This circumstance is probably no accident and is a consequence of choosing the parameters to maximize the largest LE. The eigenvalues of the equilibrium satisfy the Shilnikov condition [22] for the existence of chaos since the magnitudes of the real eigenvalues (0.3342 and 1.0319) are greater than the magnitude of the real part of the complex eigenvalue (0.0414).

3.4. Bifurcations

The routes to chaos were examined by introducing a bifurcation parameter s that multiplies the off-diagonal elements of the a_{ij} matrix in equation (1), $a_{ij} \to s a_{ij}$ for $i \neq j$. This parameter can be viewed as a measure of the species coupling since $s = 0$ decouples the equations into a

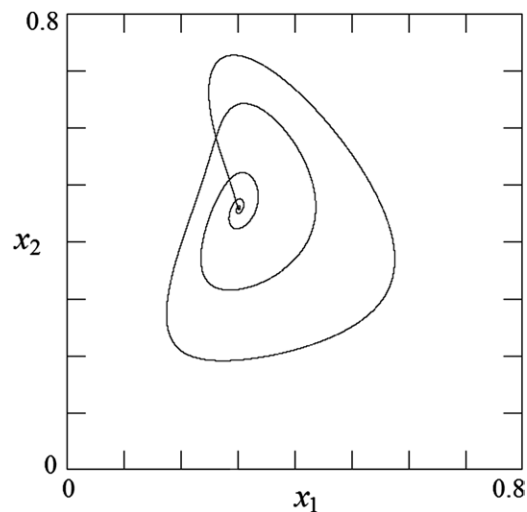**Figure 5.** Homoclinic connection projected onto the $x_1 x_2$ plane.

nonlinear system of N independent Verhulst equations which are asymptotic to $x_i = 1$ for all i. For $s = 1$, the chaotic solution described in section 3.2 is obtained. As $s \to \infty$, competition becomes increasingly severe, and all but the species with the highest growth rate ($i = 3$) die. Figure 6 shows a bifurcation diagram for successive maxima of x_1 for increasing s over the range $0.8 < s < 1.4$ and the corresponding largest LE.

The coexisting equilibrium $\bar{x}$ becomes unstable through a Hopf bifurcation at $s \approx 0.8185$, producing a limit cycle that undergoes successive period doublings, culminating in chaos. The homoclinic tangency appears to occur when the equilibrium point (which moves with s) lies on the attractor (at $s \approx 1.0001$, rather than precisely at $s = 1.0$). This value of s was determined by lengthy calculations of the trajectory on the attractor for various values of s and determining that there was a minimum approach of the trajectory to the equilibrium point and that on either side of this minimum the value of $\bar{x}_1$ has a different sign. This condition corresponds approximately to the value at which the largest Lyapunov has its maximum value. Chaos persists with embedded periodic windows until about $s \approx 1.216$, where an inverse period-doubling cascade begins. Q_{124} is stable in the small window $s \approx 1.04$ to $s \approx 1.12$, while Q_{34} becomes stable at $s \approx 1.08$, and its basin of attraction expands until it touches the growing limit cycle in a boundary crisis at $s \approx 1.31$. The bifurcation diagram exhibits hysteresis in that once s is increased to a point where Q_{34} is the only attractor ($1.31 < s < 1.4$), the trajectory remains at that attractor until s is lowered below 1.08 and Q_{34} is unstable (not shown). What appears to be a second lower branch of the bifurcation diagram that onsets around $s = 0.96$ in figure 6 is just a harmonic of the dominant frequency where the attractor develops an additional local maximum in x_1.

While figure 6 displays a sequence of attractors for a particular route through parameter space and for a particular choice of initial conditions, it does not address the possibility of multiple coexisting attractors or identify all the global bifurcations that might occur even along this route. Figure 7 shows a method for finding coexisting attractors in the range $0.8 < s < 1.4$ and their bifurcations. It consists of defining a measure, in this case the sum of the variances
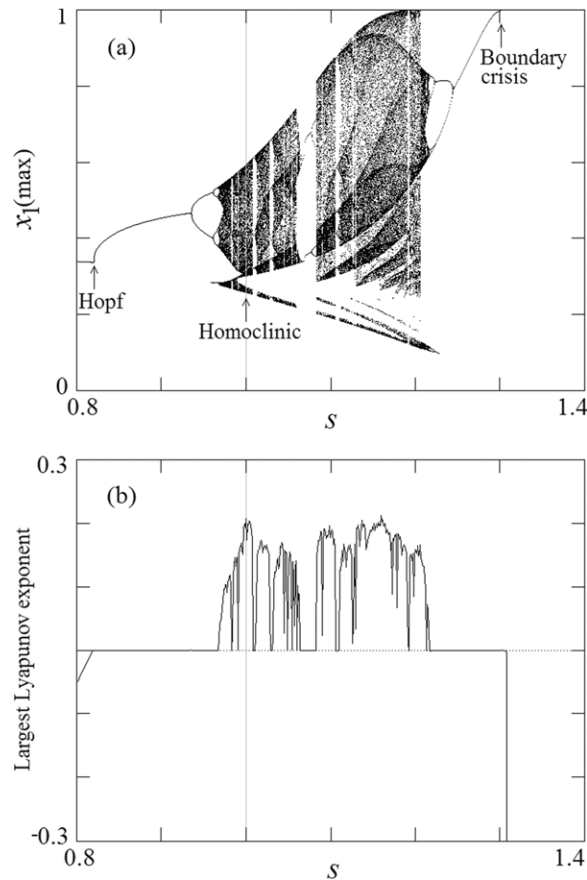
Figure 6. (*a*) Bifurcation diagram showing successive maxima of x_1 as the coupling variable s is increased and (*b*) the corresponding largest LE.

$\Sigma \sigma_i^2$ of the four variables, where

$$\sigma_i^2 = \lim_{t \to \infty} \frac{1}{t} \int_0^t (x_i - \bar{x}_i)^2.$$

The assumption is that distinct attractors are highly unlikely to have exactly the same value of this or most any other such measure. The measure will not work if there are certain symmetries in the system, but such symmetries are unlikely given the asymmetric parameters in equation (3). A Monte Carlo search of the space of several thousand initial conditions in the range $0 < x_i(0) < 1$ revealed ranges of s where the measure takes on multiple distinct values, indicating coexisting attractors, including coexisting limit cycles at $s = 1.06875$ and a limit cycle coexisting with the strange attractor at $s = 1.2375$. A by-product of the method is quantifying the size of the respective basins of attraction by keeping track of the relative probabilities of the different values of the measure.

4. Symbolic dynamics

To understand better the dynamics of this system, we break the phase space ($x_i \geqslant 0$) into $2^4 = 16$ chambers corresponding to regions where x_i is increasing/decreasing and track which
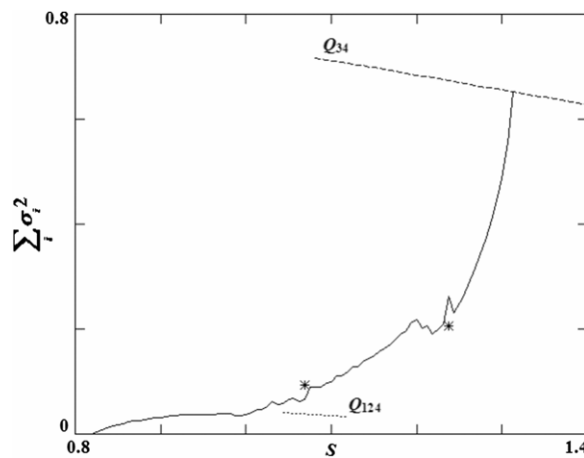
Figure 7. This Monte Carlo scan over the space of initial conditions attempted to locate coexisting attractors in the range $0.8 < s < 1.4$. The average variance of each variable was calculated along every orbit and summed. Significant differences in the variances for a single value of the bifurcation parameter s indicated multiple attractors. The fixed point Q_{124} is stable in the window $s \approx 1.04$ to $s \approx 1.12$, while Q_{34} becomes stable at $s \approx 1.08$ and is the only attractor for $1.31 < s < 1.4$. Hysteresis occurs as the orbit remains at Q_{34} even if s is lowered below 1.31 until Q_{34} becomes unstable. At $s = 1.06875$ there are coexisting limit cycles and at $s = 1.2375$ the strange attractor coexists with a limit cycle, indicated by the single points (*).

Table 1. Labelling scheme for chambers. A 0 denotes $\dot{x}_i > 0$ while a 1 denotes $\dot{x}_i < 0$.

Symbol	$\dot{x}_1$	$\dot{x}_2$	$\dot{x}_3$	$\dot{x}_4$
A	0	0	0	0
B	1	0	0	0
C	0	1	0	0
D	1	1	0	0
E	0	0	1	0
⋮	⋮	⋮	⋮	⋮
N	1	0	1	1
O	0	1	1	1
P	1	1	1	1

transitions are observed. Using 0 to denote an increasing value, 1 to denote a decreasing value and taking x_1 as the least significant bit and x_4 as the most significant bit, we can order the 16 chambers and label them sequentially from A to P (see table 1).

Two chambers, namely chamber (A), which contains the origin, and chamber (P), the unbounded chamber containing the point at infinity, have all orbits exiting and thus do not appear in any of the transitions observed on the attractor. The remaining 14 chambers can be broken into two categories: eight of which have either three species increasing and one species decreasing (e.g. B, C, etc) or three species decreasing and one species increasing (e.g. H, L, etc) and six of which have two species increasing and two decreasing (e.g. D, F, etc). There are a total of $8 \times 3 = 24$ transitions possible from the former chambers and $6 \times 4 = 24$ transitions from the latter, giving a total of 48 possible transitions.

Numerically, the trajectory on the attractor only visits 12 of the 16 chambers and undergoes 20 of the possible 48 transitions, as shown in figure 8.
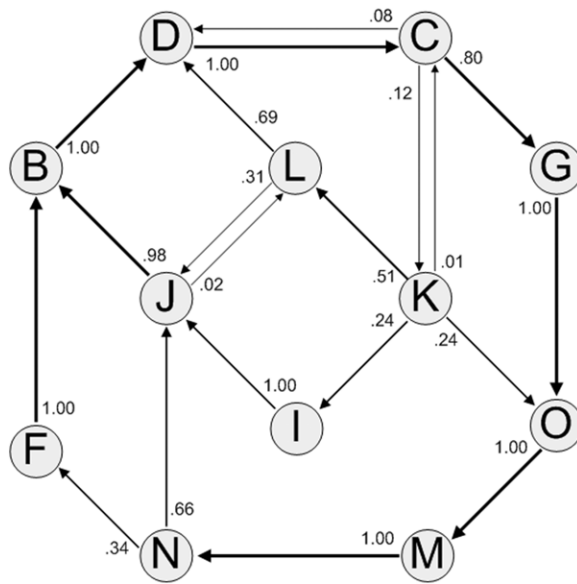
Figure 8. Graph of symbolic dynamics of the attractor. The observed probabilities of the transitions are also indicated.

Armed with a symbolic dynamic, one can compute the average Shannon entropy (*ASE*), which is a measure of rate of loss of information from a dynamic system and determines whether the system is random or regular. The *ASE* will be positive for random dynamics and zero for regularity. We denote an orbit (transition sequence) as $O_n = (A_n A_{n-1} \ldots A_1)$, where A_i may be any of the allowed symbols, and the probability of a particular orbit as $P(O_n)$. The *ASE* is given by

$$ASE = \lim_{n \to \infty} L_n \equiv \lim_{n \to \infty} \left(\frac{-1}{n} \sum_{O_n} P(O_n) \ln(P(O_n)) \right). \tag{5}$$

If the symbolic dynamics are created from a partition of phase space that maximizes the *ASE*, then the *ASE* converges to the Kolmogorov–Sinai entropy (*KSE*) of the system [29]. The *KSE* for chaotic systems is equal to the sum of the positive LEs (LE) according to Pesin's identity [30, 31]. This equivalence is intuitive. $(KSE)^{-1}$ measures the approximate number of symbols before the system is unpredictable and $(LE)^{-1}$ measures the approximate time before the system is unpredictable. When normalized by the average time between transitions, the two measures are equivalent.

For weakly chaotic systems, $LE \ll 1$, the *ASE* converges very slowly and poses a difficult computational problem. An equivalent expression [32] that converges more quickly than equation (5) for systems that exhibit a memory shorter than the time represented by n symbols is

$$ASE = \lim_{n \to \infty} \Lambda_n \equiv \lim_{n \to \infty} [(n + 1)L_{n+1} - nL_n]. \tag{6}$$

Calculation of equation (5) to a sequence length $n = 82$ converged to an *ASE* of 0.0178 as shown in figure 9. This *ASE* value is 13% lower than the sum of positive LEs, 0.0203, implying that our symbolic dynamic does not maximize the *ASE* of the system, and hence the *ASE* is not equal to the *KSE*. A phase-space encoding scheme works well for maps where the
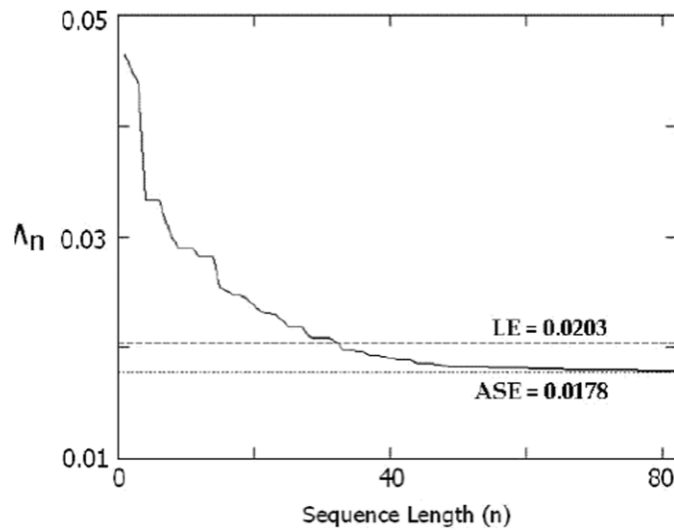
Figure 9. The plot of Λ_n showing convergence to 0.0178, a close approximation to the ASE for the symbolic dynamics.

transition rate is constant, but it needs to be modified for flows. We believe that choosing a symbolic dynamic that includes time structure would maximize the *ASE* for this system, but computational challenges accompanying this change have prevented a direct verification. The convergence of the *ASE* to a positive value is nevertheless an indication of chaos.

The seeming convergence of the *ASE* near a sequence length $n = 82$ is fortunate because this is the limit of our computational ability. In an effort to lessen further the computational load for computing the *ASE*, other approaches are possible. Figure 8 indicates that the transition (CGOMN) can be reduced to (CN), and (NFBDC) to (NC), without loss of information. The only chamber to which C transitions is G, the only chamber to which G transitions is O, etc. It turns out that these two transition sequences happen very frequently and constitute a significant portion of any sequence. If one removes the redundant transitions, the (GOM) in (CGOMN) and (FBD) in (NFBDC), a sequence that once had length $n = 82$ is now shorter. A reduced sequence of length $n' = 82$ has an actual length of $n > 82$ before reduction, and we now have the computational ability to handle longer sequences and therefore larger chunks of information.

After removing the redundant transitions from the symbol sequence, the *ASE* converged to the same value of 0.0178, confirming our intuition that entropy is a measure of information. Since no information was lost in removing the redundant symbols, the entropy did not change.

5. Self-organized criticality

One curious feature of the model is that it exhibits a power-law variation of various quantities, implying a scale-invariance as would characterize self-organized criticality [33]. For example, consider the volatility defined as

$$v(t) = \left(\frac{\sum \dot{x}_i(t)}{\sum x_i(t)} \right)^2 .$$

Here the denominator is the total biomass (or stock market average in a financial model), and the numerator is its rate of change. The volatility is large when the biomass is rapidly
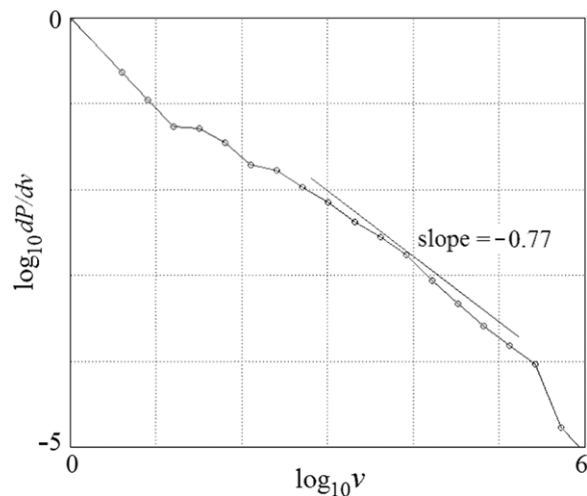
Figure 10. Probability distribution function of volatility showing a power-law scaling (arbitrary scales).

changing, and small otherwise. Figure 10 shows a plot of the probability distribution function $dP(v)/dv$ versus v obtained by following the trajectory for a time of about 10^5 with a step size of 0.01 (10^7 points) from a single initial condition and collecting the values in bins of constant logarithmic width (a factor of 2 in v). The slope is nearly constant on a log–log scale with a value of about -0.77 over some five decades of v. Other quantities such as power spectral density also show a power law, although typically over a more narrow range. The apparent occurrence of self-organized criticality in this system warrants further investigation.

6. Prevalence of chaos

Chaotic solutions are relatively rare in the vast parameter space of possible species characteristics. For example, choosing the growth rates r_i and the off-diagonal terms of the competition matrix a_{ij} randomly from an exponential distribution with mean 1.0 produces chaotic solutions (as evidenced by a LE greater than 0.001) in only about one in a hundred thousand cases for $N = 4$. Figure 11 shows the distribution of largest LEs for a large collection of such systems. The most probable dynamic is one in which the largest LE is small and negative. Most solutions result in the death of one or more species, reducing the dimension to a value where chaos is not possible or more rarely, a coexisting static equilibrium or stable limit cycle, perhaps after a period of transient chaos. For $N > 4$, the probability of finding a chaotic solution by randomly guessing is smaller still.

7. Summary and conclusions

The results presented here represent a case study of chaos in a simple Lotka–Volterra model of four species competing for a common fixed resource. It represents a highly exceptional example in which the solutions are chaotic. If we are to believe that solutions of this type are relevant to natural systems, such as in ecology or finance, there must be a more efficient mechanism for evolving such solutions out of the myriad of possibilities. There is no lack of candidates. It may be that chaotic solutions arise naturally as a result of evolution in which
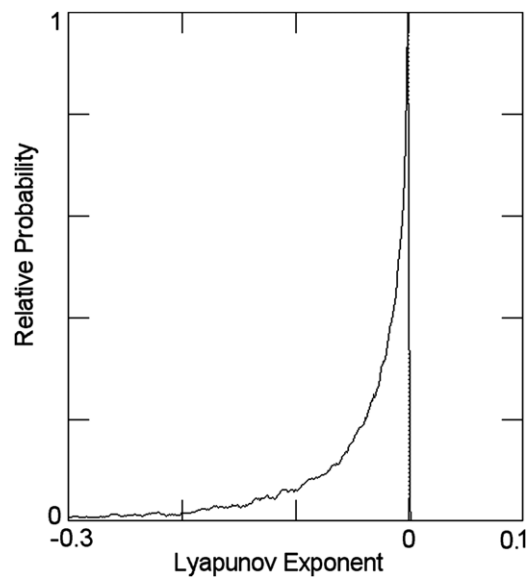
Figure 11. Probability of the largest LE, showing the rarity of chaos.

species are constantly changing their characteristics [34]. The numerical method used to find and optimize the solution presented here is one possibility. It involves a variant of simulated annealing, in which the parameter space is sampled randomly, but each time a solution is found with a LE larger than one previously found, the search is centred on a Gaussian neighbourhood of that point, and the neighbourhood size is slowly decreased. Once a chaotic solution is found, it is relatively robust to perturbations of modest size as figure 6 attests.

Although this method works satisfactorily for $N = 4$, it does not scale very well to the high N values typical of natural systems. Instead, it is possible to employ a deterministic rule, in which species adapt by selectively lowering those matrix elements that contribute most strongly to their extinction whenever their population drops below some threshold, while at the same time raising all the other values to represent adaptive learning of the surviving species [35]. This method has been used to produce chaotic systems with N as large as 400. A characteristic of these systems is that they exhibit coexistence with weakly chaotic dynamics (sometimes called the 'edge of chaos'). Interesting questions about such systems include whether self-organized criticality is common and whether the networks evolve towards one that is scale-free in the sense that the connection strengths have a power-law distribution. These issues warrant further study.

References

[1] Lotka A J 1958 *Elements of Mathematical Biology (formerly published under the title Elements of Physical Biology)* (New York: Dover)
[2] Volterra V 1926 *Mem. Acad. Lincei.* **2** 31
[3] Murray J D 1993 *Mathematical Biology vol 19 of Biomathematics* 2nd edn (Berlin: Springer)
[4] McArthur R H 1970 *Theor. Pop. Biol.* **1** 1
[5] Smale S 1976 *J. Math. Biol.* **3** 5
[6] Hirsch M 1982 *SIAM J. Math. Anal.* **13** 167
[7] Hirsch M 1985 *SIAM J. Math. Anal.* **16** 423
[8] Hirsch M 1988 *Nonlinearity* **1** 51
[9] Hirsch M 1990 *SIAM J. Math. Anal.* **21** 1225
[10] Hirsch M 1989 *J. Diff. Eqns* **80** 94
[11] Hirsch M 1991 *Ergod Theory Dyn. Syst.* **11** 443
[12] Arneodo A, Coullet P and Tresser C 1980 *Phys. Lett.* A **79** 259
[13] Arneodo A, Coullet P, Peyraud J and Tresser C 1982 *J. Math. Biol.* **14** 153
[14] Verhulst P F 1845 *Noveaux Memoires de l'Academie Royale des Sciences et Belles-Lettres de Bruxelles* **18** 1
[15] May R M 1972 *Nature* **238** 413
[16] Hirsch M W, Smale S and Devaney R L 2004 *Differential Equations, Dynamical Systems, and an Introduction to Chaos* (New York: Elsevier)
[17] Zeeman M L 1996 On directed periodic orbits in three-dimensional competitive Lotka–Volterra systems *Proc. International Conf. on Differential Equations and Applications to Biology and to Industry (Claremont, CA, 1– 4 June 1994)* ed M Martelli, K Cooke, E Clumberbatch, B Tang and H Thieme (Singapore: World Scientific) pp 563–72
[18] Zeeman M L 1993 *Dyn. Stab. Syst.* 1993 **8** 189
[19] van den Driessche P and Zeeman M L 1998 *SIAM J. Appl. Math.* **58** 227
[20] May R M and Leonard W J 1975 *SIAM J. Appl. Math.* **29** 243
[21] Coste J, Peyraud J and Coullet P 1979 *SIAM J. Appl. Math.* **36** 516
[22] Shilnikov L P 1965 *Sov. Math.—Dokl.* **6** 163
[23] Rössler O E 1976 *Phys. Lett.* A **57** 397
[24] Benettin H, Galgani L, Giorgilli A and Strelcyn J 1980 *Meccanica* **15** 9
[25] Shimada I and Nagashima T 1979 *Prog. Theor. Phys.* **61** 1605
[26] Kaplan J L and Yorke J A 1978 Functional differential equations and approximations of fixed points *Proc. Summer School and Conf. (Univ. Bonn, Bonn, 1978)* (*Lecture Notes in Mathematics* vol 730) (Berlin: Springer) pp 228–37
[27] Grassberger P and Procaccia I 1983 *Phys. Rev. Lett.* **50** 346
[28] Sprott J C and Rowlands G 2001 *Int. J. Bifurcation Chaos Appl. Sci. Eng.* **11** 1865
[29] Alekseev V M and Yakobson M V 1981 *Phys. Rep* **75** 290
[30] Pesin Y B 1977 *Usp. Mat. Nauk* **32** 55
[31] Oono P Y 1978 *Theor. Phys.* **70** 1944
[32] Gyrgyi P S G 1985 *Phys. Rev.* A **31** 3477
[33] Bak P 1996 *How Nature Works: the Science of Self-Organized Criticality* (New York: Copernicus)
[34] Sprott J C 2004 *Phys. Lett.* A **325** 329
[35] Sprott J, Vano J, Wildenberg J, Anderson M and Noel J K 2005 *Phys. Lett.* A **355** 207